

A new numerical scheme for improved Boussinesq equations with surface pressure

Deniz Bayraktar & Serdar Beji

Faculty of Naval Architecture and Ocean Engineering, Istanbul Technical University, Maslak, Istanbul, Turkey

In this work an improved Boussinesq model with a surface pressure term is discretized by a new approach. By specifying a single parameter the proposed discretization enables the user to run the program either in the long wave mode without dispersion terms or in the Boussinesq mode. Furthermore, the Boussinesq mode may be run either in the classical Boussinesq mode or in the improved Boussinesq mode by setting the dispersion parameter appropriately. In any one of these modes it is possible to specify a fixed or a moving surface pressure for simulating a moving object on the surface. The numerical model developed here is first tested by comparing the numerically simulated solitary waves with their analytical counterparts. The second test case concerns the comparison of the numerical solutions of moving surface pressures with the analytical solutions of the long wave equations for all possible modes (long wave, classical, and improved Boussinesq).

1 INTRODUCTION

The earliest depth-averaged wave model that included weakly dispersive and nonlinear effects was derived by Boussinesq (1871), in which the non-hydrostatic pressure was linearized and included in the momentum equations. The original equations were derived for constant depth only. Later, Mei and LeMehaute [1], Peregrine [2] derived Boussinesq equations for variable depth. While Mei and LeMehaute used the velocity at the bottom as the dependent variable, Peregrine used the depth-averaged velocity and assumed the vertical velocity varying linearly over the depth. Due to wide popularity of the equations derived by Peregrine, these equations are often referred to as the standard Boussinesq equations for variable depth in the coastal engineering community. The standard Boussinesq equations are valid only for relatively small kh and H/h values where kh and H/h represents the parameters indicating the relative depth (dispersion) and the wave steepness (nonlinearity), respectively. Madsen et al [3] and Madsen and Sørensen [4] included higher order terms with adjustable coefficients into the standard Boussinesq equations for constant and variable water depth, respectively. Beji and Nadaoka [5] gave an alternative derivation of Madsen et al's [4] improved Boussinesq equations. Liu & Wu [7] presented a model with specific applications to ship waves generated by a moving pressure distribution in a rectangular and trapezoidal channel by using boundary integral method. Torsvik [9] presented a numerical investigation on waves generated by

a pressure disturbance moving at constant speed in a channel with a variable cross-channel depth profile by using Lynett et al [8] and Liu & Wu [7]'s COULWAVE long wave model. The surface disturbance may come from a moving free surface object, bottom movement, or a moving object in between. The first case is associated with a moving surface pressure which is the main problem to be investigated in this study using Beji and Nadaoka's [5] alternative derivation. First of all the numerical model is verified for different test cases, such as comparing the numerically simulated solitary waves with their analytical counterparts. Then numerical solutions of all possible modes (long wave, classical, and improved Boussinesq) for moving pressures are compared with the analytical solutions. The work is currently being carried out to extend the scheme to 2-D case with realistic surface pressure forms so that waves generated by ship-like objects may be simulated.

2 IMPROVED BOUSSINESQ EQUATIONS

Dispersion relation of Peregrine's system [2] is an accurate approximation to Stokes first order wave theory for very small values of the dispersion parameter μ . Madsen et al [3] improved dispersion characteristics of this system by adding extra dispersive terms to the momentum equations as expressed in terms of depth integrated velocities $P = (h + \eta)\bar{u}$ and $Q = (h + \eta)\bar{v}$. The form of the dispersion relation is determined by matching the

dispersion characteristics to linear wave theory. Later, this procedure has been extended to the case of variable depth by Madsen and Sørensen [4]. Alternatively, Beji and Nadaoka [5] introduced a slightly different method to improve the dispersion characteristics by a simple algebraic manipulation of Peregrine's work for variable depth.

2.1 Derivation of Beji and Nadaoka's improved Boussinesq equations

Following the procedure given by Peregrine [2] the continuity and momentum equations are,

$$\frac{\partial \bar{u}}{\partial t} + (\bar{u} \cdot \nabla) \bar{u} + g \nabla \eta = \frac{1}{2} h \frac{\partial}{\partial t} \nabla [\nabla \cdot (h \bar{u})] - \frac{1}{6} h^2 \frac{\partial}{\partial t} \nabla (\nabla \cdot \bar{u}) \quad (1)$$

$$\frac{\partial \eta}{\partial t} + \nabla \cdot [(h + \eta) \bar{u}] = 0 \quad (2)$$

According to Beji and Nadaoka the second order terms are replaced with their equivalents in the Boussinesq type equations as these equations are the result of an ordering process with respect to two parameters, which are ε and μ^2 . As given by Beji and Nadaoka [5] a simple addition and subtraction in [equation \(2\)](#) gives

$$\begin{aligned} \mathbf{u}_t + (\mathbf{u} \cdot \nabla) \mathbf{u} + g \nabla \eta &= (1 + \beta) \frac{h}{2} \nabla [\nabla \cdot (h \mathbf{u}_t)] \\ &\quad - \beta \frac{h}{2} \nabla [\nabla \cdot (h \mathbf{u}_t)] - (1 + \beta) \frac{h^2}{6} \nabla (\nabla \cdot \mathbf{u}_t) \\ &\quad + \beta \frac{h^2}{6} \nabla (\nabla \cdot \mathbf{u}_t) \end{aligned} \quad (3)$$

where β is a scalar to be determined from the dispersion relation. Instead of a full replacement, a partial replacement of the dispersion terms are made so a form with better dispersion characteristics is obtained. Using $\mathbf{u}_t = -g \nabla \eta$ for replacing the terms proportional to β gives

$$\begin{aligned} \mathbf{u}_t + (\mathbf{u} \cdot \nabla) \mathbf{u} + g \nabla \eta &= (1 + \beta) \frac{h}{2} \nabla [\nabla \cdot (h \mathbf{u}_t)] \\ &\quad + \beta g \frac{h}{2} \nabla [\nabla \cdot (h \nabla \eta)] - (1 + \beta) \frac{h^2}{6} \nabla (\nabla \cdot \mathbf{u}_t) \\ &\quad - \beta g \frac{h^2}{6} \nabla (\nabla^2 \eta) \end{aligned} \quad (4)$$

which is a momentum equation with mixed dispersion terms. Setting $\beta = 0$ recovers the original

equation, while $\beta = -1$ corresponds to replacing \mathbf{u}_t with $-g \nabla \eta$ in [equation \(2\)](#). [Equations \(2\)](#) and [\(4\)](#) constitute the improved Boussinesq Equations.

2.2 Specification of dispersion parameter

Linearized 1-D Boussinesq Equations for mildly varying depth is formulated as follows. The continuity equation in expanded form

$$\frac{\partial \eta}{\partial t} + \frac{\partial h}{\partial x} u + h \frac{\partial u}{\partial x} = 0 \quad (5)$$

The momentum equation can be expanded as

$$\frac{\partial u}{\partial t} + g \frac{\partial \eta}{\partial x} = h \frac{\partial h}{\partial x} \frac{\partial^2 u}{\partial x \partial t} + \frac{h^2}{3} \frac{\partial^3 u}{\partial x^2 \partial t} \quad (6)$$

where $h \frac{\partial h}{\partial x} \frac{\partial^2 u}{\partial x \partial t}$ is the linear shoaling term while $h^2/3 \frac{\partial^3 u}{\partial x^2 \partial t}$ is the linear dispersing term. Linearized 1-D Boussinesq Equations for constant depth simplify to the following equations.

$$\frac{\partial \eta}{\partial t} + h \frac{\partial u}{\partial x} = 0 \quad (7)$$

$$\frac{\partial u}{\partial t} + g \frac{\partial \eta}{\partial x} = \frac{h^2}{3} \frac{\partial^3 u}{\partial x^2 \partial t} \quad (8)$$

Combining [equations \(6\)](#) and [\(7\)](#) by cross-differentiation the 1-D Boussinesq equations for constant depth is obtained as

$$\frac{\partial^2 \eta}{\partial t^2} - gh \frac{\partial^2 \eta}{\partial x^2} = \frac{h^2}{3} \frac{\partial^4 \eta}{\partial x^2 \partial t^2} \quad (9)$$

where $h^2/3 \frac{\partial^4 \eta}{\partial x^2 \partial t^2}$ is the linear dispersion depth. Water waves of different wave lengths travel with different phase speeds, a phenomenon known as frequency dispersion. For the case of infinitesimal wave amplitude, the terminology is linear frequency dispersion. The frequency dispersion characteristics of a Boussinesq-type of equation can be used to determine the range of wavelengths for which it is a valid approximation. Assume $\eta = \eta_0 e^{i(kx \pm \omega t)}$ so that $\eta_{tt} = -\omega^2 \eta_0 e^{i(kx \pm \omega t)}$, $\eta_{xx} = -k^2 \eta_0 e^{i(kx \pm \omega t)}$ and $\eta_{xxtt} = k^2 \omega^2 \eta_0 e^{i(kx \pm \omega t)}$. Substituting these expressions into [equation \(9\)](#) gives

$$\omega^2 \left(1 + \frac{k^2 h^2}{3} \right) = gh k^2 \quad (10)$$

which can be rewritten as,

$$\omega^2 = \frac{k^2}{1 + \frac{k^2 h^2}{3}} gh \simeq k^2 \left(1 - \frac{k^2 h^2}{3} \right) gh \quad (11)$$

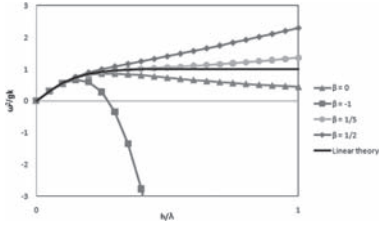


Figure 1. Dispersion curves for various values of dispersion parameter β compared with linear theory.

since $(1 + \mu^2)^{-1} \approx 1 - \mu^2$ for small values of μ^2 . Since $\omega = kc$,

$$c^2 = gh \left(1 - \frac{k^2 h^2}{3} \right) \quad (12)$$

Here $k^2 h^2 / 3$ shows the correction to the wave celerity due to the inclusion of the weak dispersion effect. Considering the improved Boussinesq equations, in linearized forms equations (2) and (4) yield the following dispersion relation evaluated by Beji and Nadaoka [5]:

$$\frac{\omega^2}{gk} = \frac{kh(1 + \beta k^2 h^2 / 3)}{[1 + (1 + \beta)k^2 h^2 / 3]} \quad (13)$$

where ω is the wave frequency, $k^2 = k_x^2 + k_y^2$ and k_x, k_y are the components of the wave number vector. Equation (13) is specified according to matching the resulting dispersion relation with a second order Padé expansion of the linear theory dispersion and β is determined from this second order Padé expansion of the linear theory dispersion relation $\omega^2 / gk = \tanh kh$:

$$\frac{\omega^2}{gk} = \frac{kh + k^3 h^3 / 15}{1 + 2k^2 h^2 / 5} \quad (14)$$

In order that Equation (13) be identical with Equation (14) β should be set to $1/5$. Figure 1 compares various values of dispersion parameters with the exact expression of linear theory. Among these asymptotic expansions, the one corresponding the Padé type expansion is the best. Thus, when $\beta = 1/5$, the model may propagate relatively shorter waves ($h/\lambda = 1$) with acceptable errors in amplitude and celerity.

3 A NEW DISCRETIZATION SCHEME FOR 1-D IMPROVED BOUSSINESQ EQUATIONS

The finite difference method is the most natural way of solving a PDE directly in an approximate

manner. The idea behind this is to discretize the continuous time and space into a finite number of discrete grid points and then to approximate the local derivatives at these grid points with finite difference schemes. For numerical modeling, the discretization of the variables u , v and η are necessary in order to solve momentum and continuity equations. Arakawa C grid which is shown in Figure 2, is the most appropriate system since it enables the discretization of the continuity equation in the most accurate manner. Here, u and η represent the horizontal velocity and the free surface displacement respectively. The surface displacement is obtained from a semi-explicit discretization of the continuity equation which is,

$$\eta_t + \frac{\partial}{\partial x}[(h + \eta)u] = 0 \quad (15)$$

Multiplying both sides of the continuity equation by Δt and differentiating with respect to x gives:

$$\begin{aligned} \left(\frac{\partial \eta}{\partial x} \right)_i^{k+1} &= \left(\frac{\partial \eta}{\partial x} \right)_i^k \\ &- \frac{1}{2} h \left[\left(\frac{\partial^2 u}{\partial x^2} \right)_{i-\frac{1}{2}}^{k+1} + \left(\frac{\partial^2 u}{\partial x^2} \right)_{i-\frac{1}{2}}^k \right] \Delta t \\ &- 2h_x \left(\frac{\partial u}{\partial x} \right)_{i-\frac{1}{2}}^{k+\frac{1}{2}} \Delta t - \frac{\partial^2}{\partial x^2} \left(\eta_i u_{i-\frac{1}{2}} \right)^{k+\frac{1}{2}} \Delta t \end{aligned} \quad (16)$$

where k denotes the time level. It should be noted that this equation is centered at $\eta_i^{k+1/2}$.

The momentum equation which is solved for u is

$$\begin{aligned} u_t + uu_x + g\eta_x &= (1 + \beta) \frac{h^2}{3} u_{xxt} \\ &+ (1 + \beta) h h_x u_{xt} \\ &+ \beta g \frac{h^2}{3} \eta_{xxx} + \beta g h h_x \eta_{xx} \end{aligned} \quad (17)$$

Discretization of the momentum equation is given as follows noting that all spatial derivatives are centered at the grid point where u_i^k is located.

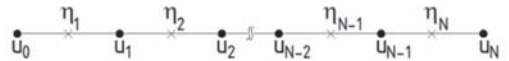


Figure 2. The Arakawa-C grid.

$$\begin{aligned}
& \frac{u_i^{k+1} - u_i^k}{\Delta t} + \frac{1}{2} g \left[\left(\frac{\partial \eta}{\partial x} \right)_{i+\frac{1}{2},j}^{k+1} + \left(\frac{\partial \eta}{\partial x} \right)_{i+\frac{1}{2},j}^k \right] \\
&= (1 + \beta) \frac{h^2}{3} \\
& \quad \left[\frac{(u_{i+1}^{k+1} - 2u_i^{k+1} + u_{i-1}^{k+1}) - (u_{i+1}^k - 2u_i^k + u_{i-1}^k)}{\Delta x^2 \Delta t} \right] \\
& \quad + (1 + \beta) h h_x \left[\frac{(u_{i+1}^{k+1} - u_{i-1}^{k+1}) - (u_{i+1}^k - u_{i-1}^k)}{2 \Delta x \Delta t} \right] \\
& \quad - u_i^{k+\frac{1}{2}} \left(\frac{\partial u_i}{\partial x} \right)^{k+\frac{1}{2}} \\
& \quad + \beta g \frac{h^2}{3} \left[\frac{\eta_{i+1}^{k+\frac{1}{2}} - 3\eta_i^{k+\frac{1}{2}} + 3\eta_{i-1}^{k+\frac{1}{2}} - \eta_{i-2}^{k+\frac{1}{2}}}{\Delta x^3} \right] \\
& \quad + \beta g h h_x \left[\frac{\eta_{i-2}^{k+\frac{1}{2}} - \eta_{i-1}^{k+\frac{1}{2}} - \eta_i^{k+\frac{1}{2}} - \eta_{i+1}^{k+\frac{1}{2}}}{2 \Delta x^2} \right] \quad (18)
\end{aligned}$$

Substituting $(\partial \eta / \partial x)_{i,j}^{k+1}$ from equation (16) into the discretized x -momentum equation (18) and multiplying by Δt gives the expression which is essentially a tridiagonal matrix system for u_{i-1}^{k+1} , u_i^{k+1} and u_{i+1}^{k+1} .

4 TEST CASES FOR THE VERIFICATION OF THE BOUSSINESQ MODEL

4.1 An analytical solution of Boussinesq equations: Solitary waves

The most elementary analytical solution of Boussinesq equations is a solitary wave. A solitary wave is a wave with only crest and a surface profile lying entirely above the still water level. It is neither oscillatory nor does it exhibit a trough. The solitary wave can be defined as a wave of translation since the water particles are displaced at a distance in the direction of wave propagation as the wave passes. A true solitary wave cannot be formed in nature because there are usually small dispersive waves at the trailing edge of the wave. On the other hand, long waves such as tsunamis and waves resulting from large displacements of water caused by such phenomena as landslides and earthquakes sometimes behave approximately like solitary waves. Also, when an oscillatory wave moves into shallow water, it may often be approximated by a solitary wave. In this situation, the wave amplitude becomes progressively higher, the crests become shorter and more pointed, and the trough becomes longer and flatter. Only one parameter, wave steepness, $\varepsilon = H/d$ is needed to specify a solitary wave because both wavelength and period of solitary waves are infinite. To the lowest order, the solitary wave profile varies as $\text{sech}^2 q$,

where $q = (3H/d)^{1/2}(x - Ct)/2d$. The free-surface elevation, particle velocities, and pressure may be expressed respectively as follows

$$\frac{\eta}{h} = \frac{u}{\sqrt{gd} \frac{H}{d}} \quad (19)$$

$$\frac{u}{\sqrt{gd}} \frac{H}{d} = \frac{\Delta p}{\rho g H} \quad (20)$$

$$\frac{\Delta p}{\rho g H} = \text{sech}^2 q \quad (21)$$

where Δp is the difference in pressure at a point under the wave due to the presence of the solitary wave. To second approximation, this pressure difference is given by

$$\frac{\Delta p}{\rho g H} = 1 - \frac{3}{4} \frac{H}{d} \left[1 - \left(\frac{Y_s}{d} \right)^2 \right] \quad (22)$$

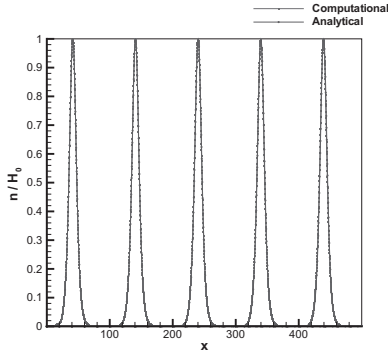
where Y_s is the height of the surface profile above the bottom. Since the solitary wave has horizontal particle velocities only in the direction of wave advance, there is a net displacement of fluid in the direction of wave propagation. The solitary wave is a limiting case of the cnoidal wave. Cnoidal waves may be viewed as the nonlinear counterparts of the sinusoidal waves in shallow water. When $k^2 = 1$, $K(k) = K(1) = \infty$, and the elliptic cosine reduces to the hyperbolic secant function and the water surface Y_s measured above the bottom reduces to

$$Y_s = d + H \text{sech}^2 \left[\sqrt{\frac{3}{4} \frac{H}{d^3}} (x - Ct) \right] \quad (23)$$

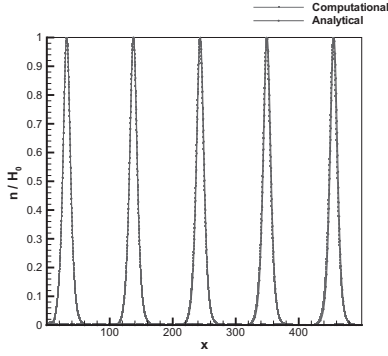
and the free surface is given by,

$$\eta = H \text{sech}^2 \left[\sqrt{\frac{3}{4} \frac{H}{d^3}} (x - Ct) \right] \quad (24)$$

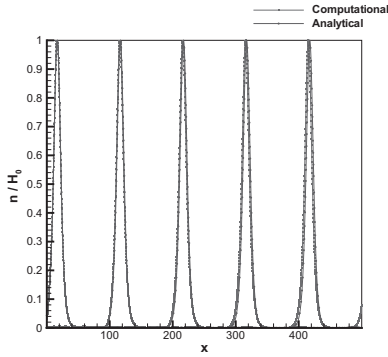
The numerical tests presented here are done using the numerical scheme developed in Section 3. The water depth is constant and both the original Boussinesq equations ($\beta = 0$) and the improved Boussinesq equations ($\beta = 1/5$) are used for simulations. As it can be seen in Figures 3 and 4 the analytical and computational results agree very well for both $\beta = 0$ and $\beta = 1/5$, although from analytical point of view, the solitary waves corresponding to the improved Boussinesq equations should be slightly different. Differences in height between analytical and computational results are shown in Figure 5 for $\beta = 0$



(a) $\beta = 0, \epsilon = 0.1$



(b) $\beta = 0, \epsilon = 0.2$



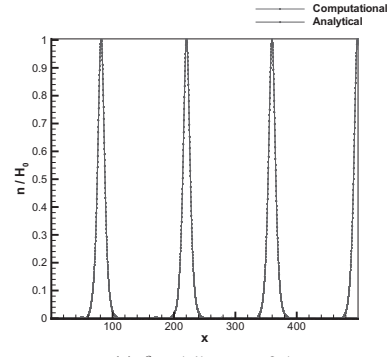
(c) $\beta = 0, \epsilon = 0.3$

Figure 3. Solitary waves for different wave heights when $\beta = 0$.

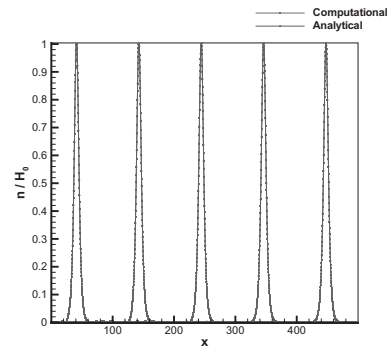
by calculating the relative error percentage for different ϵ values. It is observed that as nonlinearity parameter, ϵ , increases, the relative error percentage increases linearly up to 13% for $\epsilon = 0.4$.

4.2 Comparison of analytical solution to linear shallow water wave equations

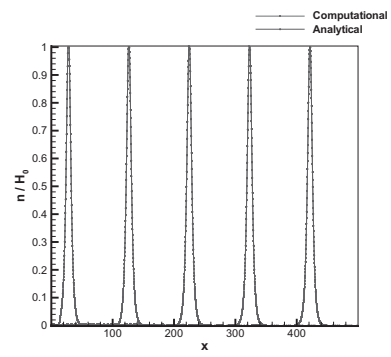
The linearized long-wave equations in 1-D in presence of a pressure term are given by,



(a) $\beta = 1.5, \epsilon = 0.1$



(b) $\beta = 1.5, \epsilon = 0.2$



(c) $\beta = 1.5, \epsilon = 0.3$

Figure 4. Solitary waves for different wave heights when $\beta = 1/5$.

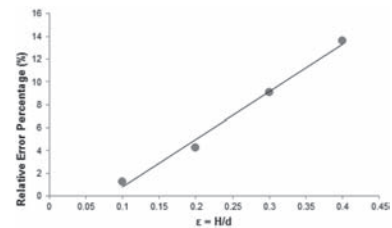


Figure 5. Relative error of the calculated wave height versus nonlinearity parameter ϵ .

$$\eta_t + hu_x = 0 \quad (25)$$

$$u_t + g\eta_x = -\frac{1}{\rho}\nabla P \quad (26)$$

where η is free surface elevation, u horizontal velocity component, P surface pressure, h constant water depth and g gravitational acceleration. Due to the moving pressure, two different free surface waves moving in opposite directions are generated. The mathematical problem can be separated as the free surface wave problem and the pressure wave problem. Assume that the moving pressure is $P = P_0 F(x - Vt)$ and for the two free waves the profiles are $\eta_1 = a_1 F(x - c_0 t)$ and $\eta_2 = a_2 F(x + c_0 t)$. Besides these free waves the forced wave profile is $\eta_3 = a_3 F(x - Vt)$ and the velocity of the forced wave is $u_3 = b_3 F(x - Vt)$. For the right moving sinusoidal wave, wave surface profile can be described as,

$$\eta = a_0 \sin(kx - \omega t) \quad (27)$$

where a_0 is the wave amplitude, k is the wave number. Differentiating the above equation with respect to x gives

$$\eta_x = ka_0 \cos(kx - \omega t) \quad (28)$$

From the momentum [equation \(26\)](#) for the unforced free wave case (no pressure) $u_t = -g\eta_x$. Substituting η_x into this expression

$$u_t = -gka_0 \cos(kx - \omega t) \quad (29)$$

Integrating over time, the horizontal velocity u is found as,

$$u = \frac{gk}{\omega} a_0 \sin(kx - \omega t) \quad (30)$$

where $a_0 \sin(kx - \omega t)$ represents η itself and $\omega = kc$. Substituting these expressions, the horizontal velocity is found as, $u = c\eta/h$. Therefore, right moving wave velocity is $u_1 = c_0 \eta_1/h$ and the left moving wave velocity is $u_2 = -c_0 \eta_2/h$. Now considering the forced wave case with pressure gradient and substituting η_3 into the continuity [equation \(25\)](#) by taking the time derivative, $u_3 = Va_3 F(x - Vt)/h$. Noting that $u_3 = b_3 F(x - Vt)$ gives

$$a_3 = -\frac{hP_0}{\rho(gh - V^2)} \quad (31)$$

Substituting $u_3 = b_3 F(x - Vt)$ and $P = P_0 F(x - Vt)$ into the momentum [equation \(26\)](#) by taking the derivative with respect to t and x respectively,

$u_3 = \rho g Va_3 F(x - Vt) + PF(x - Vt)/\rho v$. Noting that $u_3 = b_3 F(x - Vt)$ gives

$$b_3 = -\frac{P_0 V}{\rho(gh - V^2)} \quad (32)$$

Substituting a_3 into the expression $\eta_3 = a_3 F(x - Vt)$ results in $\eta_3 = hP_0 F(x - Vt)/\rho(gh - V^2)$. u_1 and u_2 are found by substituting η_1 and η_2 into the continuity [equation \(25\)](#) respectively. After these substitution $u_1 = a_1 c_0 F(x - c_0 t)/h$ and $u_2 = -a_2 c_0 F(x + c_0 t)/h$. The boundary conditions are,

$$u_1 + u_2 + u_3 = 0 \quad (33)$$

$$\eta_1 + \eta_2 + \eta_3 = 0 \quad (34)$$

Substituting free and forced solutions into (33) and (34) for $t = 0$ and solving for a_1 and a_2 gives

$$a_1 = \frac{hP_0(c_0 + V)}{2c_0\rho(gh - V^2)} \quad (35)$$

$$a_2 = \frac{hP_0(c_0 - V)}{2c_0\rho(gh - V^2)} \quad (36)$$

Finally, for three different wave profiles the following expressions for η are obtained.

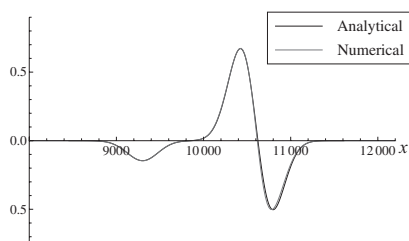
$$\eta_1 = \frac{hP_0(c_0 + V)}{2c_0\rho(gh - V^2)} F(x - c_0 t) \quad (37)$$

$$\eta_2 = \frac{hP_0(c_0 - V)}{2c_0\rho(gh - V^2)} F(x + c_0 t) \quad (38)$$

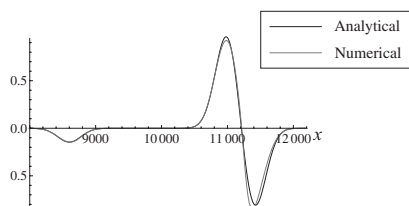
$$\eta_3 = -\frac{hP_0}{\rho(gh - V^2)} F(x - Vt) \quad (39)$$

The corresponding velocities are computed likewise. Let's assume that the moving pressure field is represented by $F(\chi) = \text{Exp}[-(\chi/250)^2]$ where $\chi = x - Vt$. In this case we choose, $h = 20 \text{ m}$, $P_0 = -4905$, $g = 9.81 \text{ m/s}^2$ and $\rho = 1000 \text{ kg/m}^3$. The length of the computational domain is 20000 m , grid size is 20 m and time step is 1 s . Solutions for linear shallow water waves at $t = 50$ and 100 s and for the velocities, $V = 10$ and 18 m/s are in [Figure 6](#).

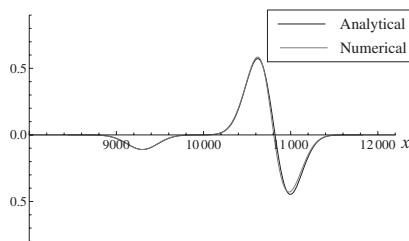
The same analytical solution is compared with one dimensional Boussinesq model when $\beta = 1/5$ for the velocities $V = 0, 10$ and 18 m/s at $t = 50$ and 100 s . As it can be seen from [Figure 7](#), the analytical and numerical solutions are again in agreement.



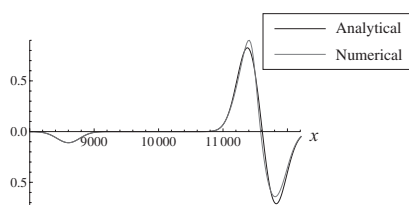
(a) $t = 50$ s, $v = 10$ m/s



(b) $t = 100$ s, $v = 10$ m/s



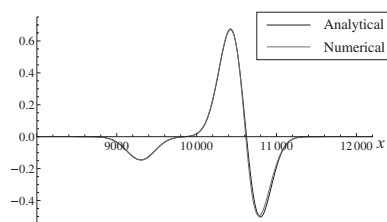
(c) $t = 50$ s, $v = 18$ m/s



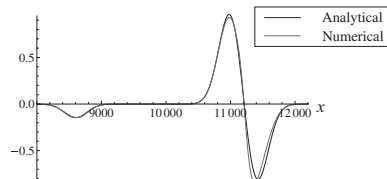
(d) $t = 100$ s, $v = 18$ m/s

Figure 6. Comparison of numerical and analytical solutions of linear shallow water waves generated by a moving pressure at $t = 50$ s and $t = 100$ s.

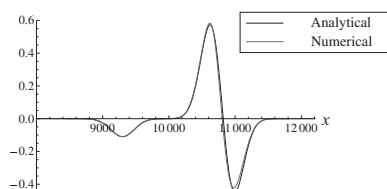
In Figure 8 the average (using 500 points) error percentages between analytical and computational results are shown for five different surface elevations for $V = 5, 10, 15, 20$ and 25 m/s which corresponds to depth Froude numbers, $0.4, 0.7, 1.1, 1.4$ and 1.8 at $t = 50$ s when $\beta = 1/5$. Results show that around Froude number 1, the relative error percentage takes its maximum value and as Froude number exceeds 1, the error percentage decreases.



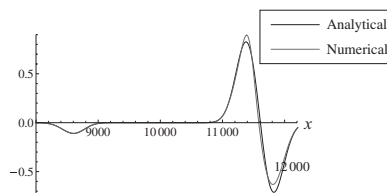
(a) $t = 50$ s, $v = 10$ m/s



(b) $t = 100$ s, $v = 10$ m/s



(c) $t = 50$ s, $v = 18$ m/s



(d) $t = 100$ s, $v = 18$ m/s

Figure 7. Comparison of analytical solution with linear shallow water waves and 1-D Boussinesq solution generated by a moving pressure when $\beta = 1/5$ at $t = 50$ s and $t = 100$ s.

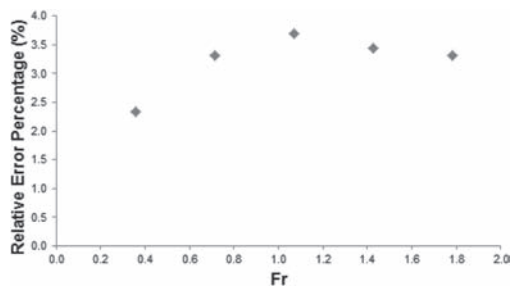


Figure 8. Average relative error of the calculated and analytical surface elevation versus Froude number.